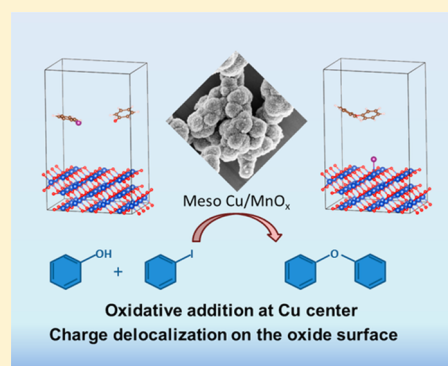


Ullmann Reaction Catalyzed by Heterogeneous Mesoporous Copper/Manganese Oxide: A Kinetic and Mechanistic Analysis

Kankana Mullick,[†] Sourav Biswas,^{†,§} Chiho Kim,[‡] Ramamurthy Ramprasad,[‡] Alfredo M. Angeles-Boza,^{*,†} and Steven L. Suib^{*,†,‡}[†]Department of Chemistry, University of Connecticut, U-3060, 55 North Eagleville Road, Storrs, Connecticut 06269, United States[‡]Institute of Materials Science, University of Connecticut, U-3060, 97 North Eagleville Road, Storrs, Connecticut 06269, United States

Supporting Information

ABSTRACT: A heterogeneous copper oxide supported on mesoporous manganese oxide (meso Cu/MnO_x) was explored for Ullmann-type cross-coupling reactions. An inverse micelle-templated evaporation-induced self-assembly method with in situ addition of copper was adopted to synthesize the mesoporous catalyst. Broad substrate scope and excellent functional group tolerability in C–O, C–N, and C–S bond formation reactions were observed using the optimized reaction conditions. The catalytic protocol was ligand free, and the catalyst was reusable without any significant loss of activity. The kinetic and Hammett analyses provided evidence for oxidative addition to a Cu(I) reaction center followed by nucleophilic addition and reductive elimination at the active copper oxide surface. Rate acceleration was observed for aryl halides with electron-withdrawing groups. The Hammett analysis determined $\rho = +1.0$, indicative of an oxidative addition, whereas the electronic effect in the phenol ring ($\rho = -2.9$) was indicative of coordination to a metal ion. Theoretically, the oxidative addition of the aryl halides is assisted by the ligand environment of the copper center. Relevant mechanistic implications are discussed on the basis of the experimental and computational results.



1. INTRODUCTION

Construction of C–heteroatom (O, N, and S) bonds is considered a popular and powerful technique by synthetic chemists due to the potential applications in the synthesis of pharmaceuticals, polymers, and natural products.^{1–7} The copper-catalyzed Ullmann-type condensation reaction is an attractive methodology due to the lower cost and decreased toxicity of copper in comparison to classic palladium catalysts used for coupling of C–O bonds.^{8,9} The traditional method developed by Fritz Ullmann and Irma Goldberg a century ago relied upon stoichiometric copper and very high reaction temperatures.¹⁰ This reaction is now known as the “classical Ullmann reaction”. Over the last decade, catalytic protocols for copper-mediated Ullmann ether coupling has been explored and improved, although most catalysts that accelerate this reaction are typically used under homogeneous reaction conditions.^{1–3,11–14} Heterogeneous copper-based catalysts for Ullmann-type condensation reactions, however, may evolve as a more suitable system because of crucial advantages such as easy separation of products, recyclability, and high stability of catalysts.¹⁵ In 2007, Lipshutz et al. reported microwave-assisted Cu/C (copper-in-charcoal)-promoted diaryl ether synthesis in the presence of 1,10-phenanthroline.¹⁶ In subsequent years several heterogeneous copper catalysts have been explored and some of the systems include copper oxide and ferrite nanoparticles,⁷ copper powder,¹⁷ copper fluorapatite,¹⁸ CuO

supported on N-doped carbon (meso-N-C-1),¹⁹ Cu/ligand catalyst immobilized on silica,⁸ Cu-Fe-hydroxalite,²⁰ magnetite-supported copper (nanocat-Fe-CuO) nanoparticles,²¹ alumina-supported CuO,²² and CuI immobilized on MOF.²³ Unfortunately, many of these systems displayed limited or narrow substrate scope. Moreover, none of the reports described mechanistic studies that might lead to a rational catalyst design for future Ullmann condensation catalysts.

Since the original work of Ullmann and Goldberg, several mechanistic investigations have been performed on homogeneous systems in order to identify the actual catalytic copper species and reaction pathway.¹⁴ On the basis of systematic investigations, up to four different pathways have been proposed to be involved in copper-catalyzed Ullmann-type condensation reactions. Interestingly, the three stable oxidation states of copper, namely Cu(I), Cu(II), and Cu(III), have been proposed.^{12,24–26} In some proposed mechanisms, the oxidation state of the copper ion changes throughout the catalytic cycle, whereas in other proposals, the oxidation state remains the same.¹⁴ It is very likely that, akin to many other catalytic systems, the reaction mechanism, including the presence or absence of changes in oxidation states, depends on the reaction conditions as well as the catalyst.

Received: May 9, 2017

Table 1. Optimization of Cross-Coupling of Phenol and Iodobenzene^a

entry	solvent	temp (°C)	base	molar ratio	conversn ^b (%)	selectivity ^b (%)	TOF ^c (h ⁻¹)
1	acetonitrile	80	K ₂ CO ₃	1/0.8	0	0	0
2	1,4-dioxane	100	K ₂ CO ₃	1/0.8	0	0	0
3	toluene	110	K ₂ CO ₃	1/0.8	0	0	0
4	DMF	140	K ₂ CO ₃	1/0.8	72	100	4.0
5 ^d	DMF	140	K ₂ CO ₃	1/0.8	2	100	0.23
6 ^e	DMF	140	K ₂ CO ₃	1/0.8	35	100	0.97
7	DMF	140	K ₂ CO ₃	1/1	30	100	1.67
8	DMF	140	K ₂ CO ₃	1/1.2	20	100	1.12
9	DMF	140	none	1/0.8	0	0	0
10	DMF	140	KOH	1/0.8	0	0	0

^aReaction conditions unless specified otherwise: phenol (1.0 mmol), iodobenzene (0.8 mmol), meso Cu/MnO_x (3 mol % Cu), solvent (5 mL), base (1.5 mmol), 6 h. ^bConversions and selectivity were determined by GC-MS on the basis of the concentration of limiting reagent. The selectivity refers to the percentage of product (aryl ether) formed with respect to the limiting reagent (iodobenzene derivatives, except entry 8, where phenol is the limiting reagent). ^cTOF = moles of limiting reagent converted per mole of catalyst per unit of time. ^d1.5 mol % Cu loading. ^e6 mol % Cu loading.

Mesoporous nanostructured materials show great potential as supports in heterogeneous catalytic applications.²⁷ Their high surface area and narrow pore size distribution make them ideal candidates as catalyst supports. Moreover, the tunable pore size and excellent adsorption properties provide good flexibility to the diffusion of reactant and products during the reaction. In 2013, a new series of mesoporous materials (University of Connecticut (UCT) mesoporous materials) was reported.²⁸ The UCT materials were synthesized by an inverse micelle templated self-assembly method. Mesoporous manganese oxide materials synthesized by this method display excellent performance in heterogeneous oxidative reactions.^{29–31} With the UCT materials synthesis approach, we recently reported mesoporous copper supported manganese oxide materials for the coupling of alkynes under aerobic conditions.³² A synergistic cooperative effect between the copper and manganese was established, where copper acts as active sites and manganese oxides as a catalyst support and electron mediator. Herein, we describe the application of our recently disclosed mesoporous copper supported manganese oxide material (meso Cu/MnO_x) as a catalyst for Ullmann-type cross-coupling reactions. High turnover numbers, excellent reusability, avoidance of ligand additives, and diversity of the coupling reactions are the notable features of our catalytic protocol. Finally, we used computational studies and kinetic analyses to formulate a reaction mechanism cycle that initiates with the oxidative addition of the aryl iodide to the meso Cu/MnO_x surface. We propose a key role of O atoms in the atom transfer processes that lead to the formation of cross-coupling products.

2. EXPERIMENTAL SECTION

2.1. Synthesis of Mesoporous Cu/MnO_x. The synthesis was performed by following the synthesis procedure of inverse micelle templated University of Connecticut (UCT) mesoporous materials.³² Copper nitrate (Cu(NO₃)₂·3H₂O) was selected as the dopant source in the synthesis. In a 120 mL beaker were placed 0.02 mol of Mn(NO₃)₂·6H₂O, 0.002 mol of Cu(NO₃)₂·3H₂O, and (0.134 mol, 10 mol %) of 1-butanol. To this solution were added 0.0034 mol of P123 (PEO₂₀PPO₇₀PEO₂₀, molar mass 5750 g mol⁻¹) and 0.032 mol of concentrated HNO₃, and the mixture was stirred at room temperature until the solution became clear. The resulting clear blue solution was then kept in an oven at 120 °C for 3 h under air. The black material was washed with excess ethanol, centrifuged, and dried in a vacuum oven overnight. The dried black powder was then subjected to a heat treatment of 150 °C for 12 h and cooled to room temperature, followed by heating at 250 °C for 3 h under air.

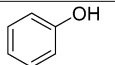
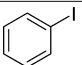
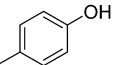
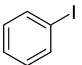
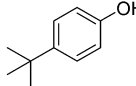
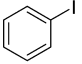
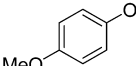
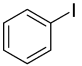
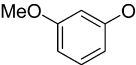
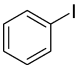
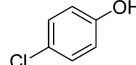
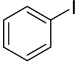
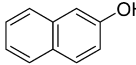
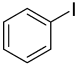
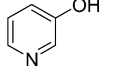
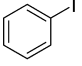
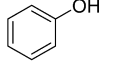
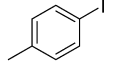
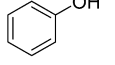
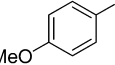
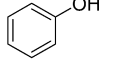
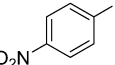
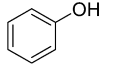
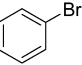
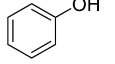
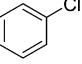
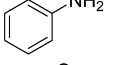
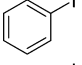
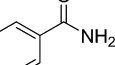
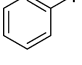
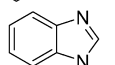
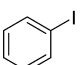
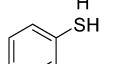
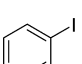
2.2. Catalytic Activity Measurements. In a typical reaction, phenol (1.0 mmol), iodobenzene (0.8 mmol), meso Cu/MnO_x (3 mol % of Cu with respect to limiting reagent), K₂CO₃ (1.5 mmol), and DMF (5 mL) were placed in a 25 mL round-bottom flask (two-necked flask for time-dependent study, where the second neck was used as a sample port). The flask with the reaction mixture and a reflux condenser was immersed in a silicon oil bath preheated to 140 °C. The reaction mixture was refluxed with vigorous stirring (700 rpm) for the required time under air. After the reaction, the mixture was cooled, the catalyst was removed by filtration, and GC-MS (gas chromatography–mass spectrometry) was used to analyze the filtrate. The conversions were determined on the basis of the concentration of limiting reagent. The analyses were performed with a 7820A GC system connected with a 5975 series MSD thermal conductivity detector from Agilent Technologies and a nonpolar cross-linked methyl siloxane column with dimensions of 12 in × 0.200 mm × 0.33 μm.

2.3. Computational Methods. Our computations were performed using density functional theory (DFT) as implemented in the Vienna ab initio smulation package (VASP),³³ the projector augmented-wave (PAW)³⁴ formalism, and the Perdew–Burke–Ernzerhof (PBE) exchange–correlation approximation.³⁵ The basis set included all of the plane waves with kinetic energies up to 450 eV. A Monkhorst–Pack grid of 2 × 2 × 1 was used for *k*-point sampling.^{36,37}

3. RESULTS

3.1. Optimization of Reaction Conditions. In order to investigate the optimum reaction conditions, aryl ether formation from phenol and iodobenzene was selected as a model reaction. First, the reaction was carried out in solvents having various polarities and boiling points (entries 1–4, Table 1). *N,N*-Dimethylformamide (DMF), which has substantial polarity and a high boiling point (153 °C), emerged as the most suitable solvent (entry 4, Table 1). Variation of conversion of phenol with catalyst loading was established for meso Cu/MnO_x (entries 4–6, Table 1). No ether formation was observed without any catalyst or using bare meso MnO_x, which signified that copper is the active site for the present cross-coupling reaction. A much lower conversion (2%) was achieved at very low copper loading (1.5 mol % Cu), whereas conversion decreased (35%) significantly at higher copper loading (6 mol % Cu). The higher adsorption of reactant or product may be the reason behind the lower activity at higher catalyst amounts (entry 6, Table 1). The copper loading of 3 mol % was found to be optimum in terms of conversion (72%) and turnover numbers (entry 4, Table 1). Furthermore, relative molar ratios of phenol to iodobenzene were tuned (entries 4, 7,

Table 2. Ullmann Cross-Coupling Reactions by Meso Cu/MnO_x^a

Entry	Nucleophiles	Aryl halides	Time (h)	Conv. ^b (%)	Selectivity ^b (%)	TON
1			20	88	>99	29.3
2 ^c			6	95	>99	31.7
3			20	97	>99	32.3
4			3	26 ^d	>99	0.87
5			20	90	>99	30.0
6			20	97	>99	32.3
7			20	67	>99	22.3
8			20	85	>99	28.3
9			20	66	>99	22.0
10			20	76	>99	25.3
11			1	>99	>99	33.3
12			20	70	>99	23.3
13			20	0	nd	0
14			20	5	90	1.67
15			20	45	>99	15.0
16			20	73	>99	24.3
17 ^c			20	89	>99	29.7

^aReaction conditions: phenol (1.0 mmol), iodobenzene (0.8 mmol), K₂CO₃ (1.5 mmol), DMF (5 mL), catalyst (3 mol % Cu), 140 °C. nd = not determined. ^bThe selectivity refers to the percentage of product (aryl ether) formed with respect to the limiting reagent. ^cUnder a nitrogen atmosphere. ^dThe excess reagent 4-methoxyphenol was totally consumed in 3 h.

and 8, Table 1) to establish that the best percent conversion was achieved with a molar ratio of 1/0.8 among phenol and iodobenzene. The presence of base was necessary (entry 9, Table 1) for activation of phenol, and K₂CO₃ was used for this reason. KOH (entry 10, Table 1) did not work, probably because of poor solubility in the solvent.

3.2. Synthetic Scope. Having determined the correct combination of solvent, base, and temperature to obtain a high TON for aryl ether synthesis, we aimed to explore the behavior of the meso Cu/MnO_x system with diverse C–O, C–N, and C–S substrates. First, derivatives of phenol were reacted

(entries 1–8, Table 2) with iodobenzene to evaluate the synthetic scope of diaryl ether formation. Phenols bearing electron-donating (entries 2–5, Table 2) and electron-withdrawing groups (entry 6, Table 2) reacted with iodobenzene to form the corresponding diaryl ether with excellent conversion (90 to >99%) and selectivity (mostly >99%). Phenols having electron-donating groups (entries 2 and 4, Table 2) reacted much more quickly in comparison to phenols having electron-withdrawing groups (entry 6, Table 2). In the case of 4-methylphenol, a small amount of oxidative products of the methyl group were observed (entry 2, Table 2). The position of

substituents resulted in significant differences in activity (entries 4 and 5, Table 2), which signifies the effect of the electronic nature of the substituent on the reaction rate. No dehalogenated product was detected in the case of phenols with chloro substitution (entry 6, Table 2). The catalyst was also useful for a reaction with a relatively bulky phenolic (1-naphthol) system (entry 7, Table 2). Heterocyclic compounds can also be effectively coupled with iodobenzene with the present protocol (entry 8, Table 2).

The catalyst also exhibited high conversions and selectivity when structurally different iodobenzenes were selected as substrates (entries 9–11, Table 2). In contrast to phenols, in the presence of iodobenzenes bearing electron-donating groups (entries 9 and 10, Table 2), much lower conversions were achieved even after longer reaction times (20 h). On the other hand, a nitro-substituted (electron-withdrawing) iodobenzene gave quantitative conversion in 1 h of reaction (entry 11, Table 2). Bromobenzene as a substrate also produced the corresponding diaryl ether with excellent conversion (70%) and selectivity (>99%) (entry 12, Table 2). However, the reaction was totally inactive for the case of chlorobenzene as the halogen-substituted benzene substrate (entry 13, Table 2).

To expand the scope of our methodology, we also performed cross-coupling between aniline, imidazole, amide, and thiophenol with iodobenzene for the respective N- and S-coupled products. A low conversion (5%) was achieved for aniline (entry 14, Table 2), whereas imidazole and amide gave moderate conversion (45–60%) but excellent selectivity (>99%) (entries 15 and 16, Table 2). On the other hand, the reaction between thiophenol and iodobenzene resulted in high conversion (89%). However, small amounts of disulfide were formed due to oxidation of thiophenol (entry 17, Table 2).

3.3. Heterogeneity and Reusability. Steady reusability and negligible leaching of active species are two important factors for an efficient heterogeneous catalytic system. We selected cross-condensation of 4-methoxyphenol and 4-nitroiodobenzene as the model reaction for a reusability study. After the reaction, the catalyst was retrieved by filtration and was washed with excess solvent, water, and ethanol (>90% recovery). Prior to reuse the catalyst was reactivated at 250 °C for 30 min to remove any adsorbed organic species. Figure S1a in the Supporting Information shows that the catalyst can retain activity and selectivity even after the fourth reuse. Moreover, no change in the PXRD pattern after the fourth cycle was observed (Figure S1b), which confirmed that the catalyst can retain the crystal structure even after multiple reuse cycles. The oxidation state of Cu was found to be 2+ by XPS after the reuse cycles, which signified the stability of our catalysts for multiple uses (Figure S1c). A hot filtration test was also carried out to verify any possible leaching of active species from the catalyst surface. No further formation of diaryl ether took place after filtering off the catalyst at 35% conversion (Figure S2 in the Supporting Information). Further, ICP analysis revealed a trace amount (1.8 ppb) of Cu in the filtrate. These results indicate that the active catalyst truly has a heterogeneous nature and highlight the sustainability of the system, since meso Cu/MnO_x can be recycled.

3.4. Kinetic and Mechanistic Study. At least four different mechanisms have been described for Ullmann-type condensation reactions (Figure 1).^{13,38} One of the proposals includes the formation of aryl radical intermediates.^{39,40} To test whether radical intermediates formed during the reaction

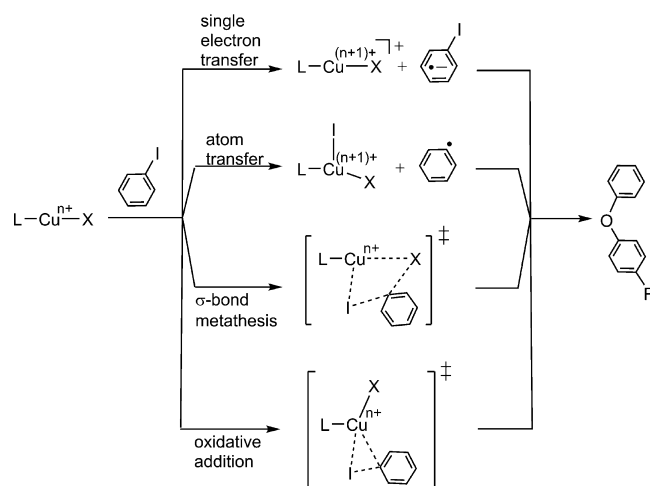


Figure 1. Possible mechanisms for Ullman cross-coupling reactions.

catalyzed by meso Cu/MnO_x, we performed the coupling reaction in the presence of a radical scavenger.

Addition of the radical scavenger phenothiazine was found to have no effect on the reaction rate of cross-condensation of phenol and iodobenzene, ruling out the formation of radical intermediates produced by homolytic cleavage of carbon–halogen bonds. As observed in Table 2, a significant difference in the reaction rate was observed due to the nature of the substituents present in iodobenzene. Linear free energy studies are powerful tools that offer chemists useful mechanistic insight. In order to test the effect of electronic changes on the step in which iodobenzene is involved, we determined the rate constants for the reaction of four different para-substituted (*p*-NO₂, *p*-H, *p*-Me, *p*-OMe) iodobenzene derivatives (Figure S3 in the Supporting Information). Continuous sampling was undertaken over the course of 1 h, and conversion and selectivity were determined by GC-MS. Kinetic experiments depicted a first-order rate equation with respect to iodobenzene derivatives. A Hammett-type analysis was used to establish the role of electronic effects of the substituents on the reaction rate (Figure S4 in the Supporting Information and Figure 2).⁴¹ In a Hammett-type analysis, a plot of logarithmic values of relative rate constants against a set of standard σ values was made.⁴¹ We plotted logarithmic values of relative rate constants against σ_p^+ ,

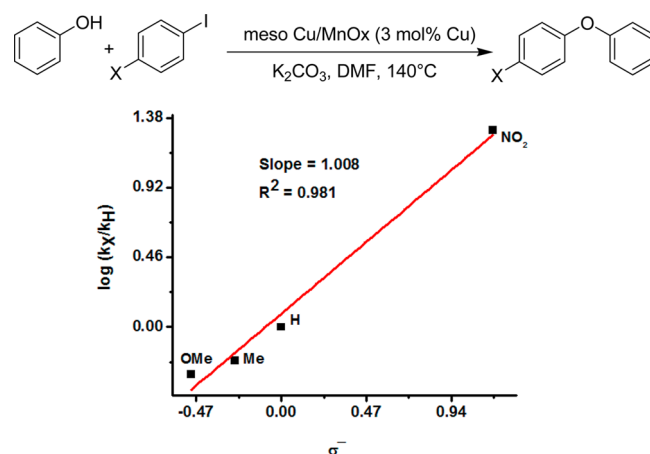


Figure 2. Hammett plot for Ullman cross-coupling reactions of para-substituted iodobenzenes. On the basis of σ^- , $\rho = 1.0$.

the Brown–Okamoto constant (Figure S4), and against σ^- values (Figure 2). Better correlation was found with the latter, although both resulted in similar ρ values: 0.92 and 1.0 for σ_p^+ and σ^- , respectively. The positive slope values suggest the development of negative charge at the reaction center.

Similarly, we performed kinetic analyses to verify the electronic influence of the substituents in the phenol derivatives (Figures S5 and S6 in the Supporting Information). The relative rates of coupling of para-substituted phenols (*p*-Cl, *p*-H, *p*-Me, *p*-OMe) were investigated. A linear relationship was found between $\log(k_X/k_H)$ and σ_p^+ (Figure 3). The slope of the

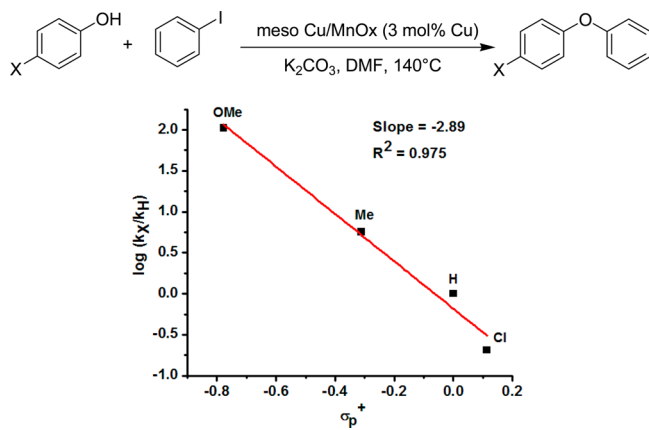


Figure 3. Hammett plot for Ullman cross-coupling reactions of para-substituted phenols. On the basis of σ_p^+ , $\rho = -2.9$.

plot shows a reaction constant ρ value of -2.9 for the phenol derivatives studied, which suggests development of a positive charge at the reaction center in the transition state involving phenol.

3.5. Computational Investigation of the Ullman Cross-Coupling Reaction Catalyzed by Meso MnO_x. To further validate the energetics during the reaction, we performed quantum mechanical computations using density functional theory (DFT). The model system was constructed with C_6H_5-O and C_6H_5-I molecules near the CuO surface. On the basis of our mechanistic studies and the literature the following reaction pathway was assumed. In step 1, the C_6H_5-O and C_6H_5-I molecules are both freestanding with the distance from the CuO surface being far enough to avoid interactions between the surface and molecules. In step 2, C_6H_5-I approaches the surface. This is followed by step 3, in which C_6H_5-O forms a bond with the surface. In step 4, oxidative addition and nucleophilic addition steps occur. Finally, in step 5, the product $C_6H_5-O-C_6H_5$ forms by reductive elimination. The energy profile for the reaction is shown in Figure 4; the structures are also shown. As observed, the system becomes stabilized as the molecules get closer to the surface. A significant decrease in the system energy was calculated for step 4, further confirming the oxidative addition to the catalyst. Interestingly, the metal ion is assisted during the oxidative addition by an oxide, with the aryl group on the latter and the iodide in the copper coordination sphere. The higher energy ($3.96 \text{ kcal mol}^{-1}$ higher) of the final product formation is due to the formation of the final product and release from the surface. The Bader analysis based charge⁴² is shown in Figure 4 with schematic representation of each reaction coordinate. No distinct change in charge on the copper atoms was observed throughout the reaction, highlighting the ability of the

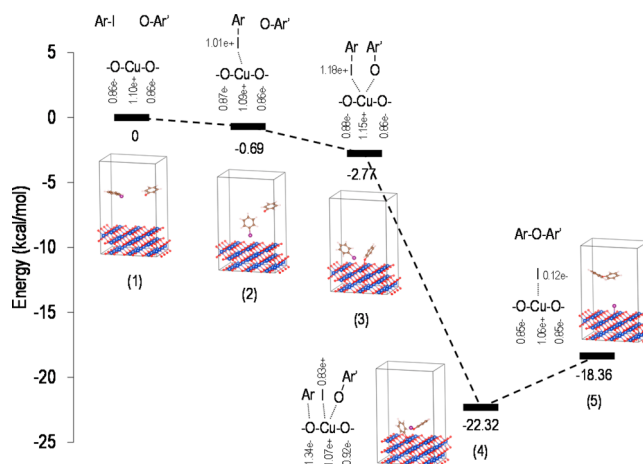


Figure 4. Change in the DFT computed energy for the reaction pathway of Ullmann coupling over a CuO surface and corresponding change in the charge associated with the atoms directly involved in the reaction.

surrounding molecules on the surface to assist in the activation of the substrates.

4. DISCUSSION

This study illustrates the use of a mesoporous copper oxide supported on manganese oxide as an efficient heterogeneous catalyst for Ullmann-type condensation reactions. An inverse micelle templated self-assembly procedure has been used to synthesize the material. A nonpolar pluronic surfactant (P123) acts as the scaffold to build the meso structure. Copper was introduced in the system by in situ addition of a copper salt during the sol–gel process. The manganese oxide acts as a support for tethering the active copper oxide nanoparticle while also preserving the mesoporosity. The synthesis of bare mesoporous copper oxide was unsuccessful using this procedure.

Our system indicates excellent substrate scope and functional group tolerance for Ullmann ether coupling reactions. Steric effects in the reaction were evaluated by using the sterically hindered phenol 2,4,6-tri-*tert*-butylphenol as one of the coupling reagents. No ether formation occurred, indicating that sterics play a role in the Ullman cross-coupling catalyzed by meso Cu/MnO_x. Meso Cu/MnO_x can also be applied to cross-coupling of aniline, imidazole, amide, and thiophenol derivatives for construction of C–N and C–S bonds. Substrates bearing heteroatoms such as S and N are known to poison transition metal oxide based catalysts due to strong coordination of the heteroatom to the transition-metal centers.⁴³ We observed decreased activity with N-containing substrates in comparison to phenol: e.g., aniline, imidazole, and amide reactions. However, 3-pyridylmethanol was coupled efficiently to the corresponding aryl ether with no significant drop in TON and selectivity in comparison to the phenol, indicating that meso Cu/MnO_x is less susceptible to poisoning than other metal oxide based catalysts. Interestingly, thiophenol displayed much higher activity (89% conversion). In the case of thiophenol, the formation of the disulfide was observed, as manganese oxide is known to oxidize thiol to disulfide.⁴⁴ Several other copper-based heterogeneous catalysts have been reported for Ullmann coupling reactions which are more active than the catalytic system presented here.^{15b–f} However, our system complements those catalysts, since at low temperature

and low catalyst loadings, the aforementioned systems were only applicable to C–O coupling^{15b–d} or suffered from poor reusability.^{15e,f} Next, we use kinetic studies to elucidate the reaction mechanism of the coupling reaction so it can be used as a benchmark to rationally design future copper-based heterogeneous catalysts.

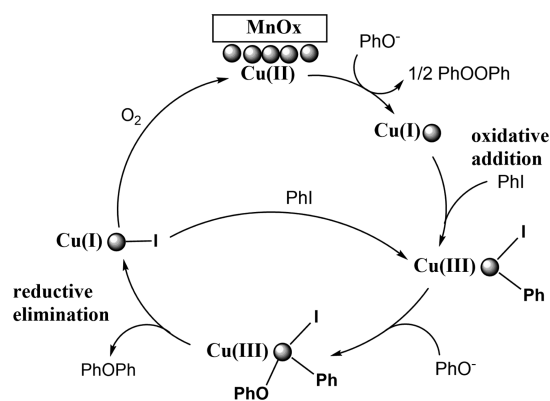
4.1. Reaction Mechanism: Evidence for a Cu(I) Species. Generally, the most accepted reaction mechanism involves oxidative addition of the haloarene to a Cu(I) center to generate an aryl–Cu(III)–X intermediate followed by nucleophilic reaction and reductive elimination to yield the desired product. Very few studies have shown isolation of the intermediates in copper-catalyzed Ullmann coupling reactions.^{25,45} The works of Buchwald and Hartwig provided evidence of formation of a Cu(I) complex with nitrogen donor ligands.^{25,26} However, no evidence of Cu(III)–aryl complex formation was observed, since reductive elimination from the Cu(III) intermediate is much more rapid than oxidative addition of the Cu(I) center. In studies by Stahl and co-workers, Cu(I)/Cu(III) redox steps have been observed, where a macrocyclic ligand has been used to stabilize the Cu(III) species.⁴⁶ Cu(II) salts have also been used as catalysts for the Ullmann reaction, although in these cases reduction to a Cu(I) species happens with the concomitant oxidation of phenoxide or amines present in the reaction mixture.^{11,12} Because of the large body of evidence pointing at the preference of Cu(I) species to initiate Ullman-type coupling reactions, we investigated whether Cu(I) formation was feasible under our reaction conditions. For this study, we used an analogous material, mesoporous Cu supported TiO₂ (prepared by the same method; see the Supporting Information for details) in this study to avoid the reoxidation of Cu(I) by Mn³⁺, as observed in our previous study.³² We treated the meso Cu/TiO₂ material with phenol in basic medium under N₂ and probed for the presence of Cu(I) using XPS. Notably, the presence of Cu(I) was confirmed under these reaction conditions (Figure S7 in the Supporting Information), likely formed by a redox reaction with phenoxide, as observed in other systems.^{11,12}

4.2. Reaction Mechanism: Evidence Favors Oxidative Addition. Our Hammett analysis shows that electron-deficient para-substituted aryl iodides facilitate more rapid turnover rates. The positive sign of the ρ value indicates a buildup of negative charge in the transition state involving iodobenzene. We obtained a better correlation against σ^- in comparison to σ_p^+ . Similar behavior, that is better correlation with σ^- over σ_p^+ , has been observed in oxidative addition reactions.⁴⁷ Thus, an oxidative addition step is likely to be present during the Ullmann ether coupling catalyzed by meso Cu/MnO_x. The oxidative additions of aryl iodides to Pd(0) and Ni(0) complexes have ρ values of 2.7 and 2.0, respectively,^{48,49} whereas a smaller value, $\rho = 0.9$, has been reported for the oxidative addition of aryl iodides to a Rh(I) complex containing a diarylamido/bis(phosphine) pincer ligand (Table S2 in the Supporting Information).⁴⁷ On the basis of these values, the meso Cu/MnO_x–aryl iodide transition state resembles more the transition state originating from the less nucleophilic Rh(I)–diarylamido/bis(phosphine) complex than that of the Pd(0) and Ni(0) species. After the oxidative addition, phenol approaches the intermediate formed by the catalyst and the aryl iodide. We observed faster reaction rates in the presence of electron-donating groups on the phenol ring (Figure 3). The negative ρ value also indicates the development of a positively

charged species in the transition state. The magnitude of ρ indicates that a phenoxy radical species is not formed, as the formation of radicals usually leads to small ρ values.⁴¹ In addition, the presence of a radical inhibitor had no effect on the reaction rate and no biphenyl was produced, reinforcing the idea that no radicals are formed during the reaction. The development of a positive charge is probable due to the coordination of phenol or phenoxide anion to the copper center.

4.3. Reaction Mechanism Proposal. We propose a mechanism for the coupling reaction catalyzed by meso Cu/MnO_x (Scheme 1). First, a catalytically active Cu(I) center is

Scheme 1. Proposed Catalytic Mechanism for the Ullmann Coupling Reaction by Meso Cu/MnO_x



generated from the Cu(II) species by reaction with phenolate ion (formed by the presence of base) as determined by XPS. The iodobenzene molecule undergoes oxidative addition to the Cu(I) oxide on the surface, resulting in the formation of Cu–I and O–aryl bonds. The oxidative addition is followed by nucleophilic addition of phenoxide ion. Finally, reductive elimination produces the desired biaryl product. The typical oxidative state changes that occurred on the copper center, e.g. Cu(I)/Cu(III) cycling, in molecular systems during the Ullman cross-coupling reaction is avoided with this catalyst because of the delocalization of the charge on the Cu/MnO_x surface. Whether the oxidative addition of aryl halide or coordination of the nucleophiles (–O, –N, or –S) happens first is a question that remains to be answered. Mechanistic studies by Buchwald and Hartwig showed formation of a Cu(I)–nucleophile bond prior to oxidative addition.^{25,26} On the other hand, the works of Monnier and Stahl confirmed that oxidative addition preceded the nucleophilic addition in some systems.^{46,50} Finally, it is well-known that the nature of the nucleophiles and ligands and the reaction conditions largely influence the mechanism of the Ullmann coupling reaction.

5. CONCLUSIONS

In summary, we report the use of the thermally stable and reusable mesoporous copper-supported manganese oxide material as a catalyst for Ullman cross-coupling reactions. We demonstrate a broad substrate scope and excellent functional group tolerability in C–O, C–N, and C–S bond formation reactions. The catalytic protocol circumvents the use of additional ligands. The catalyst was reusable without any significant loss of activity after four cycles. Our experimental and computational work provided evidence for oxidative addition of the aryl iodide substrate assisted by the O atoms

on the surface of the catalyst. Similarly to oxidative additions on single metal centers, rate acceleration in the presence of electron-withdrawing groups on the aryl halide ring is observed. The Hammett analysis indicates that the Cu–O moiety in which the aryl iodide is added acts more like a Rh(I) species than a Ni(0) or Pd(0) intermediate. Future work will focus on using experimental and computational studies to understand the oxidative addition of aryl iodides to Cu/MnO_x, test our proposal that in the current Cu/MnO_x mesoporous system the Cu(III) oxidation state is avoided due to the delocalization of the charge throughout the material, and elucidate the full mechanism of cross-coupling.

■ ASSOCIATED CONTENT

● Supporting Information

The Supporting Information is available free of charge on the ACS Publications website at DOI: 10.1021/acs.inorgchem.7b01177.

Additional experimental details and characterization data (PDF)

■ AUTHOR INFORMATION

Corresponding Authors

*E-mail for A.M.A.-B.: alfredo.angeles-boza@uconn.edu.

*E-mail for S.L.S.: steven.suib@uconn.edu.

ORCID

Sourav Biswas: 0000-0001-7368-3947

Alfredo M. Angeles-Boza: 0000-0002-5560-4405

Steven L. Suib: 0000-0003-3073-311X

Present Address

[§]S.B.: Department of Chemistry, University of Wisconsin—Madison, 1101 University Avenue, Madison, Wisconsin 53706, USA.

Notes

The authors declare no competing financial interest.

■ ACKNOWLEDGMENTS

S.L.S. acknowledges the support of the U.S. Department of Energy, Office of Basic Energy Sciences, Division of Chemical, Biological and Geological Sciences, under grant DE-FG02-86ER13622.A000. A.M.A.-B. thanks the University of Connecticut for generous start-up funds.

■ REFERENCES

- (1) Cristau, H.-J.; Cellier, P. P.; Hamada, S.; Spindler, J.-F.; Taillefer, M. A General and Mild Ullmann-Type Synthesis of Diaryl Ethers. *Org. Lett.* **2004**, *6*, 913–916.
- (2) Salih, M. Q.; Beaudry, C. M. Enantioselective Ullmann Ether Couplings: Syntheses of (–)-Myricatomentogenin, (–)-Jugathanin, (+)-Galeon, and (+)-Pterocarane. *Org. Lett.* **2013**, *15*, 4540–4543.
- (3) Haumesser, J.; Pereira, A. M. V. M.; Gisselbrecht, J.-P.; Merahi, K.; Choua, S.; Weiss, J.; Cavaleiro, J. A. S.; Ruppert, R. Inexpensive and Efficient Ullmann Methodology To Prepare Donor-Substituted Porphyrins. *Org. Lett.* **2013**, *15* (15), 6282–6285.
- (4) Hwang, J. Y.; Kawasuji, T.; Lowes, D. J.; Clark, J. A.; Connelly, M. C.; Zhu, F.; Guiguemde, W. A.; Sigal, M. S.; Wilson, E. B.; DeRisi, J. L.; Guy, R. K. Synthesis and Evaluation of 7-Substituted 4-Aminoquinoline Analogues for Antimalarial Activity. *J. Med. Chem.* **2011**, *54*, 7084–7093.
- (5) Devambatla, R. K. V.; Namjoshi, O. A.; Choudhary, S.; Hamel, E.; Shaffer, C. V.; Rohena, C. C.; Mooberry, S. L.; Gangjee, A. Design, Synthesis, and Preclinical Evaluation of 4-Substituted-5-methyl-furo[2,3-d]pyrimidines as Microtubule Targeting Agents That Are Effective against Multidrug Resistant Cancer Cells. *J. Med. Chem.* **2016**, *59*, 5752–5765.
- (6) Yang, D.; Fu, H. A Simple and Practical Copper-Catalyzed Approach to Substituted Phenols from Aryl Halides by Using Water as the Solvent. *Chem. - Eur. J.* **2010**, *16*, 2366–2370.
- (7) (a) Jammi, S.; Sakthivel, S.; Rout, L.; Mukherjee, T.; Mandal, S.; Mitra, R.; Saha, P.; Punniyamurthy, T. CuO nanoparticles catalyzed C–N, C–O, and C–S cross-coupling reactions: Scope and mechanism. *J. Org. Chem.* **2009**, *74*, 1971–1976. (b) Yang, S.; Wu, C.; Zhou, H.; Yang, Y.; Zhao, Y.; Wang, C.; Yang, W.; Xu, J. An Ullmann C–O Coupling Reaction Catalyzed by Magnetic Copper Ferrite Nanoparticles. *Adv. Synth. Catal.* **2013**, *355*, 53–58.
- (8) (a) Hassan, J.; Sévignon, M.; Gozzi, C.; Schulz, E.; Lemaire, M. Aryl–Aryl Bond Formation One Century after the Discovery of the Ullmann Reaction. *Chem. Rev.* **2002**, *102*, 1359–1470. (b) Benyahya, S.; Monnier, F.; Taillefer, M.; Man, M. W. C.; Bied, C.; Ouazzani, F. Efficient and Versatile Sol-Gel Immobilized Copper Catalyst for Ullmann Arylation of Phenols. *Adv. Synth. Catal.* **2008**, *350*, 2205–2208. (c) Guo, X.-X.; Gu, D.-W.; Wu, Z.; Zhang, W. Copper-Catalyzed C–H Functionalization Reactions: Efficient Synthesis of Heterocycles. *Chem. Rev.* **2015**, *115*, 1622–1651.
- (9) (a) Beletskaya, I. P.; Cheprakov, A. V. Copper in cross-coupling reactions: The post-Ullmann chemistry. *Coord. Chem. Rev.* **2004**, *248*, 2337–2364. (b) Evano, G.; Blanchard, N.; Toumi, M. Copper-mediated coupling reactions and their applications in natural products and designed biomolecules synthesis. *Chem. Rev.* **2008**, *108*, 3054–3131.
- (10) Ullmann, F.; Bielecki, J. Ueber Synthesen in der Biphenylreihe. *Ber. Dtsch. Chem. Ges.* **1901**, *34*, 2174–2185.
- (11) Weingarten, H. Mechanism of the Ullmann Condensation. *J. Org. Chem.* **1964**, *29*, 3624–3626.
- (12) Paine, A. J. Mechanisms and models for copper mediated nucleophilic aromatic substitution. 2. Single catalytic species from three different oxidation states of copper in an Ullmann synthesis of triarylamines. *J. Am. Chem. Soc.* **1987**, *109*, 1496–1502.
- (13) Sperotto, E.; van Klink, G. P. M.; van Koten, G.; de Vries, J. G. The mechanism of the modified Ullmann reaction. *Dalton Trans.* **2010**, *39*, 10338–10351.
- (14) Sambigiato, C.; Marsden, S. P.; Blacker, A. J.; McGowan, P. C. Copper catalyzed Ullmann type chemistry: from mechanistic aspects to modern development. *Chem. Soc. Rev.* **2014**, *43*, 3525–3550.
- (15) (a) Sheldon, R.; Downing, R. Heterogeneous catalytic transformations for environmentally friendly production. *Appl. Catal., A* **1999**, *189*, 163–183. (b) Magné, V.; Garnier, T.; Danel, M.; Pale, P.; Chassaing, S. Cu(I)-USY as a Ligand-Free and Recyclable Catalytic System for the Ullmann-Type Diaryl Ether Synthesis. *Org. Lett.* **2015**, *17*, 4494–4497. (c) Kim, J. Y.; Park, J. C.; Kim, A.; Kim, A. Y.; Lee, H. J.; Song, H.; Park, K. H. Cu₂O Nanocube-Catalyzed Cross-Coupling of Aryl Halides with Phenols via Ullmann Coupling. *Eur. J. Inorg. Chem.* **2009**, *2009*, 4219–4223. (d) Niu, F.; Jiang, Y.; Song, W. *In situ* loading of Cu₂O nanoparticles on a hydroxyl group rich TiO₂ precursor as an excellent catalyst for the Ullmann reaction. *Nano Res.* **2010**, *3*, 757–763. (e) Kidwai, M.; Mishra, N. K.; Bansal, V.; Kumar, A.; Mozumdar, S. Cu-nanoparticle catalyzed O-arylation of phenols with aryl halides via Ullmann coupling. *Tetrahedron Lett.* **2007**, *48*, 8883–8887. (f) Isomura, Y.; Narushima, T.; Kawasaki, H.; Yonezawa, T.; Obora, Y. Surfactant-free single-nano-sized colloidal Cu nanoparticles for use as an active catalyst in Ullmann-coupling reaction. *Chem. Commun.* **2012**, *48*, 3784–3786.
- (16) Lipshutz, B. H.; Unger, J. B.; Taft, B. R. Copper-in-charcoal (Cu/C) promoted diaryl ether formation. *Org. Lett.* **2007**, *9*, 1089–1092.
- (17) Jiao, J.; Zhang, X.-R.; Chang, N.-H.; Wang, J.; Wei, J.-F.; Shi, X.-Y.; Chen, Z.-G. A facile and practical copper powder-catalyzed, organic solvent-and ligand-free Ullmann amination of aryl halides. *J. Org. Chem.* **2011**, *76*, 1180–1183.
- (18) Mulla, S. A.; Inamdar, S. M.; Pathan, M. Y.; Chavan, S. S. , Ligand free, highly efficient synthesis of diaryl ether over copper

- fluorapatite as heterogeneous reusable catalyst. *Tetrahedron Lett.* **2012**, *53*, 1826–1829.
- (19) Zhang, P.; Yuan, J.; Li, H.; Liu, X.; Xu, X.; Antonietti, M.; Wang, Y. Mesoporous nitrogen-doped carbon for copper-mediated Ullmann-type C–O/N/S cross-coupling reactions. *RSC Adv.* **2013**, *3*, 1890–1895.
- (20) Jadhav, V. H.; Dumbre, D. K.; Phapale, V. B. Borate, H. B.; Wakharkar, R. D., Efficient N-arylation of amines catalyzed by Cu–Fe–hydroxalate. *Catal. Commun.* **2007**, *8*, 65–68.
- (21) Shelke, S. N.; Bankar, S. R.; Mhaske, G. R.; Kadam, S. S.; Murade, D. K.; Bhorkade, S. B.; Rathi, A. K.; Bundaleski, N.; Teodoro, O. M.; Zboril, R. Iron oxide-supported copper oxide nanoparticles (Nanocat-Fe-CuO): magnetically recyclable catalysts for the synthesis of pyrazole derivatives, 4-methoxyaniline, and Ullmann-type condensation reactions. *ACS Sustainable Chem. Eng.* **2014**, *2*, 1699–1706.
- (22) Ling, P.; Li, D.; Wang, X. Supported CuO/ γ -Al₂O₃ as heterogeneous catalyst for synthesis of diaryl ether under ligand-free conditions. *J. Mol. Catal. A: Chem.* **2012**, *357*, 112–116.
- (23) Wang, M.; Yuan, B.; Ma, T.; Jiang, H.; Li, Y. Ligand-free coupling of phenols and alcohols with aryl halides by a recyclable heterogeneous copper catalyst. *RSC Adv.* **2012**, *2*, 5528–5530.
- (24) Franc, G.; Jutand, A. On the origin of copper (i) catalysts from copper (ii) precursors in C–N and C–O cross-couplings. *Dalton Trans.* **2010**, *39*, 7873–7875.
- (25) Tye, J. W.; Weng, Z.; Johns, A. M.; Incarvito, C. D.; Hartwig, J. F. Copper complexes of anionic nitrogen ligands in the amidation and imidation of aryl halides. *J. Am. Chem. Soc.* **2008**, *130*, 9971–9983.
- (26) Strieter, E. R.; Bhayana, B.; Buchwald, S. L. Mechanistic studies on the copper-catalyzed N-arylation of amides. *J. Am. Chem. Soc.* **2009**, *131*, 78–88.
- (27) Taguchi, A.; Schüth, F. Ordered mesoporous materials in catalysis. *Microporous Mesoporous Mater.* **2005**, *77*, 1–45.
- (28) Poyraz, A. S.; Kuo, C.-H.; Biswas, S.; King'ondo, C. K.; Suib, S. L. A general approach to crystalline and monomodal pore size mesoporous materials. *Nat. Commun.* **2013**, *4*, 2952.
- (29) Biswas, S.; Poyraz, A. S.; Meng, Y.; Kuo, C.-H.; Guild, C.; Tripp, H.; Suib, S. L. Ion induced promotion of activity enhancement of mesoporous manganese oxides for aerobic oxidation reactions. *Appl. Catal., B* **2015**, *165*, 731–741.
- (30) Biswas, S.; Dutta, B.; Mullick, K.; Kuo, C.-H.; Poyraz, A. S.; Suib, S. L. Aerobic Oxidation of Amines to Imines by Cesium-Promoted Mesoporous Manganese Oxide. *ACS Catal.* **2015**, *5*, 4394–4403.
- (31) Dutta, B.; Biswas, S.; Sharma, V.; Savage, N. O.; Alpay, S.; Suib, S. L. Mesoporous Manganese Oxide Catalyzed Aerobic Oxidative Coupling of Anilines To Aromatic Azo Compounds. *Angew. Chem., Int. Ed.* **2016**, *55*, 2171–2174.
- (32) Biswas, S.; Mullick, K.; Chen, S.-Y.; Kriz, D. A.; Shakil, M.; Kuo, C.-H.; Angeles-Boza, A. M.; Rossi, A. R.; Suib, S. L. Mesoporous Copper/Manganese Oxide Catalyzed Coupling of Alkynes: Evidence for Synergistic Cooperative Catalysis. *ACS Catal.* **2016**, *6*, 5069–5080.
- (33) Kresse, G.; Hafner, J. Ab initio molecular dynamics for liquid metals. *Phys. Rev. B: Condens. Matter Mater. Phys.* **1993**, *47*, 558.
- (34) Blöchl, P. E. Projector augmented-wave method. *Phys. Rev. B: Condens. Matter Mater. Phys.* **1994**, *50*, 17953.
- (35) Perdew, J. P.; Burke, K.; Ernzerhof, M. Generalized gradient approximation made simple. *Phys. Rev. Lett.* **1996**, *77*, 3865.
- (36) Monkhorst, H. J.; Pack, J. D. Special points for Brillouin-zone integrations. *Phys. Rev. B* **1976**, *13*, 5188.
- (37) Genuino, H. C.; Dharmarathna, S.; Njagi, E. C.; Mei, M. C.; Suib, S. L. Gas-phase total oxidation of benzene, toluene, ethylbenzene, and xylenes using shape-selective manganese oxide and copper manganese oxide catalysts. *J. Phys. Chem. C* **2012**, *116*, 12066–12078.
- (38) Jones, G. O.; Liu, P.; Houk, K. N.; Buchwald, S. L. Computational Explorations of Mechanisms and Ligand-Directed Selectivities of Copper-Catalyzed Ullmann-Type Reactions. *J. Am. Chem. Soc.* **2010**, *132*, 6205–6213.
- (39) Bunnett, J. F.; Kim, J. K. Evidence for a radical mechanism of aromatic "nucleophilic" substitution. *J. Am. Chem. Soc.* **1970**, *92*, 7463–7464.
- (40) Creutz, S. E.; Lotito, K. J.; Fu, G. C.; Peters, J. C. Photoinduced Ullmann C–N coupling: demonstrating the viability of a radical pathway. *Science* **2012**, *338*, 647–651.
- (41) Johnson, C. D. *The Hammett Equation*; CUP Archive: Cambridge, U.K., 1973.
- (42) Henkelman, G.; Arnaldsson, A.; Jónsson, H. A fast and robust algorithm for Bader decomposition of charge density. *Comput. Mater. Sci.* **2006**, *36*, 354–360.
- (43) Peral, J.; Ollis, D. F. TiO₂ photocatalyst deactivation by gas-phase oxidation of heteroatom organics. *J. Mol. Catal. A: Chem.* **1997**, *115*, 347–354.
- (44) Dharmarathna, S.; King'ondo, C. K.; Pahalagedara, L.; Kuo, C.-H.; Zhang, Y.; Suib, S. L. Manganese octahedral molecular sieve (OMS-2) catalysts for selective aerobic oxidation of thiols to disulfides. *Appl. Catal., B* **2014**, *147*, 124–131.
- (45) Huffman, L. M.; Stahl, S. S. Carbon–nitrogen bond formation involving well-defined aryl–copper (III) complexes. *J. Am. Chem. Soc.* **2008**, *130*, 9196–9197.
- (46) Casitas, A.; King, A. E.; Parella, T.; Costas, M.; Stahl, S. S.; Ribas, X. Direct observation of CuI/CuIII redox steps relevant to Ullmann-type coupling reactions. *Chem. Sci.* **2010**, *1*, 326–330.
- (47) Puri, M.; Gatard, S.; Smith, D. A.; Ozerov, O. V. Competition Studies of Oxidative Addition of Aryl Halides to the (PNP)Rh Fragment. *Organometallics* **2011**, *30*, 2472–2482.
- (48) Amatore, C.; Azzabi, M.; Jutand, A. Role and effects of halide ions on the rates and mechanisms of oxidative addition of iodobenzene to low-ligated zerovalent palladium complexes Pd⁰(PPh₃)₂. *J. Am. Chem. Soc.* **1991**, *113*, 8375–8384.
- (49) Tsou, T. T.; Kochi, J. K. Mechanism of oxidative addition. Reaction of nickel(0) complexes with aromatic halides. *J. Am. Chem. Soc.* **1979**, *101*, 6319–6332.
- (50) Monnier, F.; Taillefer, M. Catalytic C–C, C–N, and C–O Ullmann-Type Coupling Reactions. *Angew. Chem., Int. Ed.* **2009**, *48*, 6954–6971.